

ONLINE PREPRINT

A Simulation-free Group Sequential Design with Max-combo Tests in the Presence of Non-proportional Hazards[†]

Lili Wang¹ | Xiaodong Luo² | Cheng Zheng²¹Department of Biostatistics, University of Michigan, Ann Arbor, Michigan, U.S.A.²Department of Biostatistics and Programming, Research and Development, Sanofi US, Bridgewater, New Jersey, U.S.A.**Correspondence**

*Cheng Zheng, Department of Biostatistics and Programming, Research and Development, Sanofi US, Bridgewater, New Jersey, U.S.A. Email: Cheng.Zheng@sanofi.com

Summary

Non-proportional hazards (NPH) have been observed recently in many immunology clinical trials. Weighted log-rank tests (WLRT) with suitably chosen weights can be used to improve the power of detecting the difference of the two survival curves in the presence of NPH. However, it is not easy to choose a proper WLRT in practice when both robustness and efficiency are considered. A versatile maxcombo test was proposed to achieve the balance of robustness and efficiency and has received increasing attentions in both methodology development and application. However, survival trials often warrant interim analyses due to its high cost and long duration. The integration and application of maxcombo tests in interim analyses often require extensive simulation studies. In this paper, we propose a simulation-free approach for group sequential design with maxcombo test in survival trials. The simulation results support that the proposed approaches successfully control both the type I error rate and offer great accuracy and flexibility in estimating sample sizes, at the expense of light computation burden. Notably, our methods display a strong robustness towards various model misspecifications, and have been implemented in an R package for free access online.

KEYWORDS:

delayed treatment effect, group sequential design, interim analysis, maxcombo, non-proportional hazard, weighted log-rank test

1 | INTRODUCTION

Survival trials are commonly used in confirmatory trials to demonstrate treatment effect in oncology. In the presence of non-proportional hazards (NPH), which is frequently encountered in practice, the detection power is much lower than those survival curves with proportional hazards (PH). For instance, delayed treatment effect was often reported in immune-directed anti-cancer therapies^{1,2}. Unlike chemotherapy, which displays early antitumor effects or separation between the survival curves, immunotherapy stimulates the patient's immune system for an antitumor response, causing delayed clinical effect³.

Weighted log-rank tests (WLRT) incorporate time-dependent weights to improve the detection power in presence of non-proportional hazards. Weight functions can be dependent on survival functions⁴ or at-risk proportions^{5,6}, etc. In this report, we focus on the Fleming-Harrington class of WLRT, but one can easily extend the proposed design to all other weights. The shape of the Fleming-Harrington weight function can be adjusted according to the survival curves: putting more weight on late

[†] A Group-sequential Design for Max-combo tests

departure for delayed effect. According to Schoenfeld⁷, the optimal weight (with highest power) should be proportional to the magnitude of the logarithm of the hazard ratio⁸, which is a time dependent function under NPH.

Survival curves are generally unknown and thus the appropriate weight function cannot be decided before starting the trial. Lee⁹ proposed a versatile max-combo test, which takes the maximum value of a set of different WLRTs to provide a robust detection. In other words, whether it is PH or NPH, the max-combo test gives power quite close to the optimal one in the combo. A typical maxcombo test combines several WLRTs, each of which is powerful in detecting certain pattern of NPH, and the multiple testing adjustment for the overall test is conducted via a Dunnett-type parametric method, with such structure, the maxcombo test. Moreover, the selected best weight reflects the true hazard ratio between the two treatment arms.

Interim analysis (IA) in group sequential design (GS) enable multiple looks (interims) before the end of the study. They will allow early stops when there is evidence to discontinue the study, like rejection of the null hypothesis, toxic effects, and futility. Though their benefits have been extensively studied to our knowledge, group sequential design with max-combo tests (GS-MC) has not been systematically studied, despite the demonstrated nice features on the max-combo tests. In this report, we develop simulation-free approaches to calculate the stopping boundaries with GS-MC design. As demonstrated in the sequel, our approaches can control type I error, and provide an efficient way to calculating power and sample size with GS-MC design.

The rest of this report is organized as follows. We introduce the designs of WLRT and max-combo test, and extend them to GS-MC in Section 2. We propose simulation-free approaches for GS-MC to compute boundaries for type I error control and practical sample size in realistic scenarios in Section 3. We evaluate the proposed methods through extensive simulations with or without violations of the model assumptions in Section 4. Some concluding remarks are provided in Section 5.

2 | PROBLEM FORMULATION

2.1 | Notation

Suppose there are n subjects entering the study at E_i , $i = 1, \dots, n$, within the accrual period $[0, R]$. Let T_i denote a univariate event time of interest, and A_i indicate treatment assignment, e.g. using 0 for control group and 1 for treatment group. Given the treatment $A_i = a$, $a \in \{1, 0\}$, event time T_i follows a survival function $S_a(s) = P(T_i > s | A_i = a)$. To consider censoring time C_i , the observed follow-up time and event indicator are $\{Y_i(t) = \min(T_i, C_i, t - E_i)\}$ and $\delta_i(t) = I(Y_i(t) = T_i)$, where t is a stopping time that plays a dual role of a right-truncation time for those who have not entered the study yet when $t < R$, and an administrative censoring time for the rest. Alternatively, observed event times can also be written in a counting process form $N_i(t, s) = I(T_i \leq s, \delta_i(t) = 1)$. Note that t and E_i follow chronological time scale, while s in all the functions, T_i and C_i are in a follow-up time scale starting from the accrual time E_i . The censoring might differ between the two treatment arms so that the survival functions of censoring are $S_{c_a}(s) = P(C_i > s | A_i = a)$.

In this report, we allow both the control and the treatment group to follow piecewise exponential distributions following a general form:

$$S_a(s) = \exp \left[- \sum_{q=1}^Q \lambda_{aq} \max \{0, \min(\epsilon_q - \epsilon_{q-1}, s - \epsilon_{q-1})\} \right], \quad a = 1, 0. \quad (1)$$

Note that $0 = \epsilon_0 < \epsilon_1 < \dots < \epsilon_Q = \infty$ are the splitting points where the hazard changes and λ_{aq} is the hazard in the interval $[\epsilon_{q-1}, \epsilon_q)$, $q = 1, \dots, Q$. The flexibility of including multiple pieces enables an accurate approximation of any shapes of survival function. For constant hazard ratio or PH, one can set either $Q = 1$ or $\lambda_{aq} = \lambda_{a1}$ for $\forall q$. The hazard ratios between the two treatment arms are $\Theta = \{\theta_q = \lambda_{1q}/\lambda_{0q}, q = 1, \dots, Q\}$. The hazard ratios can describe all different changing pattern of the treatment effects including examples like a constant effect with identical θ_q , and a delayed or increasing effect with $0 < \theta_Q < \dots < \theta_1 \leq 1$ etc. For delayed treatment effect, a simple NPH case is given in Appendix 2 (B4) and (B5) with only the two-piece exponential distribution considered: hazards are $\lambda_{11} = \lambda_{01} = \lambda$ and $\Theta_1 = 1$ for $[0, \epsilon)$, $\lambda_{12} = \Theta_2 \lambda$ and $\lambda_{02} = \lambda$ for $[\epsilon, \infty)$. For this simple case, the null hypothesis (H_0) is $\theta_2 = 1$ and the alternative hypothesis (H_1) is $\theta_2 = \theta$ with some $\theta < 1$. Or more broadly speaking, the null hypothesis H_0 is always $\Theta = \Theta_0$ with all elements $\theta_q = 1$, and the alternative one H_1 could embrace any predefined $\Theta = \Theta_1$ with at least one of elements $\theta_q \neq 1$. Additionally, we simply assume uniform accrual and only administrative right censoring at time τ for now following the proposal from Hasegawa¹⁰ in Section 3 when proposing our solutions. But the robustness of our proposed method can be seen in our simulations results in Section 4.

2.2 | Weighted log-rank test

Suppose the treatment-specific at-risk proportions are $R_a(t, s) = \frac{1}{n} \sum_{i=1}^n I(Y_i(t) \geq s, A_i = a)$, and the total at-risk proportion is $R(t, s) = R_1(t, s) + R_0(t, s)$. A standardized Fleming-Harrington class weighted log-rank test statistic (WLRT) stopped at time t can be expressed as:

$$G_{\rho, \gamma}(t) = \frac{\sum_{i=1}^n \int_0^t w_{\rho, \gamma}(s) [A_i - \frac{R_1(t, s)}{R(t, s)}] N_i(t, ds)}{\sqrt{\sum_{i=1}^n \int_0^t w_{\rho, \gamma}(s)^2 \frac{R_1(t, s) R_0(t, s)}{R(t, s)^2} N_i(t, ds)}}, \quad (2)$$

where $w_{\rho, \gamma}(s) = S(s^-)^\rho \{1 - S(s^-)\}^\gamma$ and $S(\cdot)$ is the marginal survival function averaging two treatment arms.

The denominator of the WLRT test statistic in (2) is actually the asymptotic variance estimator of the numerator, which we denote as,

$$\hat{V}(G_{\rho, \gamma}(t)) = \frac{1}{n} \sum_{i=1}^n \int_0^t w_{\rho, \gamma}(s)^2 \frac{R_1(t, s) R_0(t, s)}{R(t, s)^2} N_i(t, ds). \quad (3)$$

Regulating the two parameters ρ and γ can adjust the shape of the weights, and thus the focus of the detection. For instance, $\rho = \gamma = 0$ it becomes a standard log-rank test (SLRT), which provides best power in presence of PH; while $\rho = 0$ and $\gamma = 1$, it emphasizes more on late departures and thus provides better power for delayed effect as a special case of NPH.

Sample size calculation for a confirmatory clinical trial is based on the predefined null and alternative hypotheses (denoted by H_0 and H_1). For PH, SLRT has a close-form required event count estimator following its asymptotic distribution⁷:

$$d = \frac{(z_\alpha + z_{1-\beta})^2}{p(1-p)\Delta^2}, \quad (4)$$

where here z_α and $z_{1-\beta}$ are two critical values of standard normal distribution, and Δ is the effective difference between two arms, which can be the constant $\log(\lambda_1(t)/\lambda_0(t))$ in PH case. However, the sample size computation for WLRT was established using some stochastic process methods as suggested by Lakatos¹¹ and Hasegawa¹⁰. Suppose b is the number of intervals at each time unit (month), we let $M(t) = \text{floor}(bt)$ be the total number of time intervals at an equal length $[s_0 = 0, s_1, s_2, \dots, s_M = t]$, where t is a stopping point like the study end τ . Then there follows the mean estimator $\tilde{E}_{sto}(G_{\rho, \gamma}(t))$ and variance/information estimator of the numerator in (2):

$$\tilde{E}_{sto}(G_{\rho, \gamma}(t)) = \sum_{j=0}^{M(t)-1} D_{j, \Theta_1}^*(t) w_{\rho, \gamma}^*(j) \left[\frac{\phi_j \theta_j}{1 + \phi_j \theta_j} - \frac{\phi_j}{1 + \phi_j} \right] \quad (5)$$

$$\tilde{V}_{sto}(G_{\rho, \gamma}(t)) = \sum_{j=0}^{M(t)-1} D_{j, \Theta_1}^*(t) w_{\rho, \gamma}^*(j)^2 \frac{\phi_j}{(1 + \phi_j)^2}, \quad (6)$$

where,

$$\begin{aligned} R_1^*(0) &= p, R_0^*(0) = 1 - p, w_{\rho, \gamma}^*(j) = S(s_j)^\rho [1 - S(s_j)]^\gamma \\ R_a^*(j+1) &= R_a^*(j) \left[1 - h_a^*(s_j) \frac{1}{b} - \frac{I(s_j > \tau - R)}{b(\tau - s_j)} \right], h_a^*(s_j) = \frac{f_a(s_j)}{S_a(s_j)}, a = 0, 1 \\ \theta_j^* &= \frac{h_1(s_j)}{h_0(s_j)}, \phi_j^* = \frac{R_1^*(s_j)}{R_0^*(s_j)}, D_{j, \Theta_1}^*(t) = \left[\{h_0^*(s_j) R_0^*(j) + h_1^*(s_j) R_1^*(j)\} \frac{1}{b} \right] \min\left(\frac{t}{R}, 1\right). \end{aligned} \quad (7)$$

The subscript Θ_1 for $D_{j, \Theta_1}^*(t)$ in (5-7) above is trying to label them with their assumed hazard ratios for the two treatment arms under H_1 . In order to be consistent across the paper, we call them ‘‘predicted’’ mean and variance and denoted using accent tilde to distinguish them from those estimated using observed data following (3), which are accented with an hat. Marginal survival function can be approximated by $S(s) = (1-p)S_0(s) + pS_1(s)$. In contrast to the proposal by Hasegawa¹⁰, there is an additional multiplicative term $\min(\frac{t}{R}, 1)$ for the formulation of $D_{j, \Theta_1}^*(t)$ in (7) to account for a special case that $t < R$.

Lakatos¹¹ demonstrated that the standardized WLRT in (2) asymptotically follows a normal distribution with its variance equal 1, and its mean predicted to be

$$\tilde{\mu}_{\rho, \gamma}(t) = \frac{\tilde{E}_{sto}(G_{\rho, \gamma}(t))}{\sqrt{\tilde{V}_{sto}(G_{\rho, \gamma}(t))}}. \quad (8)$$

Having $t = \tau$, we complete the sample size computation for WLRT, in terms of either total number of subjects (n) or events (d):

$$\begin{aligned} n &= \left(\frac{z_\alpha + z_{1-\beta}}{\tilde{\mu}_{\rho, \gamma}(\tau)} \right)^2 \\ d &= n D_{\Theta_1}^*(\tau), \end{aligned} \quad (9)$$

where $D_{\Theta_1}^*(\tau) = \sum_{j=0}^{M-1} D_{j, \Theta_1}^*(\tau)$ approximates the probability of observing an event from each subject.

2.3 | Maxcombo test

In practice, however, the true survival curves or the hazard ratio between the treatment arms are usually unknown; moreover, the existence of delayed treatment effect and its severity can hardly be predicted in advance. To that end, Lee⁹ proposed a versatile max-combo test, taking the maximum of a combo of different WLRTs to cover various scenarios: PH, NPH with early, middle and late effects. The general form of a maxcombo test is

$$G_{max}(t) = \max(G_{\rho_1, \gamma_1}(t), G_{\rho_2, \gamma_2}(t), \dots, G_{\rho_K, \gamma_K}(t)), \quad (10)$$

where $G_{\rho_k, \gamma_k}(t)$ is one of the K different Fleming-Harrington family WLRTs. Boundaries calculation for a maxcombo test statistic is equivalent to finding the boundary value at the end of the study $g(\tau)$ such that

$$P(G_{max}(\tau) < g(\tau) \mid H_0) = 1 - \alpha, \quad (11)$$

where H_0 denotes the null hypothesis with $\theta = 1$, and α is the type I error. According to Lee¹², $\mathbf{G}(t) = [G_{\rho_1, \gamma_1}(t), \dots, G_{\rho_K, \gamma_K}(t)]'$ is (asymptotically) multivariate normal distributed with mean 0 and variance 1, and the correlation for $k_1 \neq k_2$

$$Cor(G_{\rho_{k_1}, \gamma_{k_1}}(t), G_{\rho_{k_2}, \gamma_{k_2}}(t)) = \frac{Cov(G_{\rho_{k_1}, \gamma_{k_1}}(t), G_{\rho_{k_2}, \gamma_{k_2}}(t))}{\sqrt{V(G_{\rho_{k_1}, \gamma_{k_1}}(t))V(G_{\rho_{k_2}, \gamma_{k_2}}(t))}}. \quad (12)$$

The variances can be obtained through either the data-driven estimation $\hat{V}(G_{\rho, \gamma}(t))$ in (3) or the stochastic prediction $\tilde{V}_{sto}(G_{\rho, \gamma}(t))$ in (6). In a similar vein, covariance can be calculated using the similar two computational approaches following the equivalence below,

$$Cov(G_{\rho_{k_1}, \gamma_{k_1}}(t), G_{\rho_{k_2}, \gamma_{k_2}}(t)) = V \left\{ G_{\frac{\rho_{k_1} + \rho_{k_2}}{2}, \frac{\gamma_{k_1} + \gamma_{k_2}}{2}}(t) \right\}. \quad (13)$$

Alternative to using the prediction based on a uniformly increasing stochastic process (denoted with subscript “sto”), the (piece-wise) exponential distributions in (1) can provide close-form predictions for all the mean, variance and covariance values we need according to exact distribution functions we presumed for tests, thus we name such prediction method as “exact prediction”, and denote those values of interest with a subscript “exa”. Please check the exactly predicted variances (\tilde{V}_{exa}) and covariance (Cov_{exa}) for the simple case with two-piece exponential survival curves in Appendix 2. The exact prediction method can largely alleviate the computational burden, though the close-form solutions may not be obtainable for complex survival functions which are not exponentially distributed. For that complicated case, one might refer to numerical approximation by transforming the integration to a summation over many small intervals, which is basically very similar to the stochastic prediction we are proposing here.

Under H_1 , the asymptotic mean for each WLRT can be approximated through (5), and thus we obtain the mean vector $\tilde{\boldsymbol{\mu}}(t) = [\tilde{\mu}_{\rho_1, \gamma_1}(t), \dots, \tilde{\mu}_{\rho_K, \gamma_K}(t)]'$. Thus the approximate asymptotic distribution of the test statistics $\mathbf{G}(t)$ is multivariate normal with mean $\sqrt{n}\tilde{\boldsymbol{\mu}}(t)$ and the covariance/correlation matrix can be obtained via the prediction methods proposed for the boundary calculation in (12). Note that we do not consider using the estimation approach for sample size calculation, since sample size calculation is usually decided before starting a trial in group sequential designs. The sample size is obtained through solving the function that the type II error equals β , i.e.,

$$P(G_{max}(\tau) < g(\tau) \mid H_1) = \beta. \quad (14)$$

2.4 | Group Sequential Design for Maxcombo tests

Interim analyses or group sequential designs are commonly seen in clinical trial, aiming to save time and budgets by stopping a trial early when there is sufficient statistical evidence to terminate the study, either due to its futility/unexpected side effects or dramatic treatment effect. Introducing maxcombo tests into group sequential design, or abbreviated as GS-MC was discussed in the FDA workshop held at Duke-Margolis Health Policy Center in 2018¹³. There were plenty of simulations showing that maxcombo would improve the robustness when the NPH existed but was unknown. For instance, when a delayed treatment effect is present, a maxcombo test of $G_{0,0}(t)$ and $G_{0,1}(t)$ has its power slightly lower than using $G_{0,1}(t)$ solely, but much higher than $G_{0,0}(t)$. Thus, GS-MC can largely reduce the sample size than using SLRT and possibly shorten the follow-up time.

There are mainly two problems that hinder the implementation of GS-MC into practice. The first is how to calculate the boundaries for each stage to control the type I errors spent at each stage, and the second is how to obtain the sample size to guarantee the power. Both two problems can be solved through extensive simulations, but the computational burden could be huge. To avoid the tedious simulations, we propose a design procedure that can control the type I and accurately predicted the required sample size by approximating the asymptotic distribution of all the test statistics across different stopping points.

3 | PROPOSED SOLUTIONS

3.1 | Correlation matrix approximation

The correlation matrix requires 3 different types of correlations. The first are within-stage correlations $Cor(G_{\rho_{k_1}, \gamma_{k_1}}(t), G_{\rho_{k_2}, \gamma_{k_2}}(t))$, and can be approximated through formulas comparable to (12). The second are the within-test correlations for arbitrary two stopping time points $0 < t_{m_1} < t_{m_2} \leq \tau$ and $m_1 < m_2$, which can be approximated by

$$Cor(G_{\rho, \gamma}(t_{m_1}), G_{\rho, \gamma}(t_{m_2})) = \sqrt{\frac{V(G_{\rho, \gamma}(t_{m_1}))}{V(G_{\rho, \gamma}(t_{m_2}))}}. \quad (15)$$

The information fraction $IF_{\rho, \gamma}(t_{m_1}, t_{m_2}) = V(G_{\rho, \gamma}(t_{m_1}))/V(G_{\rho, \gamma}(t_{m_2}))$ under the square root was also used to decide stopping times¹⁴. The equality in (15) asymptotically holds only under H_0 , since the independent increments $Cov(G_{\rho, \gamma}(t_{m_1}), G_{\rho, \gamma}(t_{m_2})) = V(G_{\rho, \gamma}(t_{m_1}))$ is asymptotically true¹⁵. However, when the difference between the two treatment arms are not extremely large with high event rates, or under the so-called ‘‘local alternatives’’, independent increments and thus the equality in (15) can be shown to be approximately true (Example 1 in Luo et al¹⁶ and simulations in Section 4). Note that the variance value for both the within-test and within-stage correlations can be obtained via both prediction and estimation approaches.

The third type are correlations that across different time points and test types. To compute the two correlations $Cor(G_{\rho_{k_1}, \gamma_{k_1}}(t_{m_1}), G_{\rho_{k_2}, \gamma_{k_2}}(t_{m_2}))$, we propose a simple calculation based on the other two types of correlations following Theorem 1, which is proved in Appendix 1.

Theorem 1. If X_1, X_2 and X_3 have mean 0, variance 1, and satisfy $X_3 = \phi X_2 + M$ where $M \perp (X_1, X_2)$ and ϕ is a constant value, it can be shown that $cor(X_1, X_3) = cor(X_1, X_2)cor(X_2, X_3)$.

In particular, we let $X_1 = G_{\rho_{k_1}, \gamma_{k_1}}(t_{m_1}) - E[G_{\rho_{k_1}, \gamma_{k_1}}(t_{m_1})]$ and $X_2 = G_{\rho_{k_2}, \gamma_{k_2}}(t_{m_1}) - E[G_{\rho_{k_2}, \gamma_{k_2}}(t_{m_1})]$. One can show that $X_3 = G_{\rho_{k_2}, \gamma_{k_2}}(t_{m_2}) - E[G_{\rho_{k_2}, \gamma_{k_2}}(t_{m_2})] = \phi X_2 + M$, where $\phi = IF_{\rho_{k_2}, \gamma_{k_2}}(t_{m_1}, t_{m_2})$ and $M = [G_{\rho_{k_2}, \gamma_{k_2}}(t_{m_2}) - G_{\rho_{k_2}, \gamma_{k_2}}(t_{m_1}) - E\{G_{\rho_{k_2}, \gamma_{k_2}}(t_{m_2}) - G_{\rho_{k_2}, \gamma_{k_2}}(t_{m_1})\}]/V(G_{\rho_{k_2}, \gamma_{k_2}}(t_{m_2}))$. Note that under the H_0 we have $E(G_{\rho, \gamma}(t)) = 0$. Moreover, $M \perp (X_1, X_2)$ is asymptotically true following the asymptotic independent increment property¹⁵ under the H_0 , but only approximately true under H_1 when the difference between two arms and the event rates are restricted within some practical range. In the Section 4, we will evaluate through extensive simulations to explore how well the this approximation approach can handle various scenarios and assumption violations. Following Theorem 1, we have:

$$\begin{aligned} Cor(G_{\rho_{k_1}, \gamma_{k_1}}(t_{m_1}), G_{\rho_{k_2}, \gamma_{k_2}}(t_{m_2})) = \\ Cor(G_{\rho_{k_1}, \gamma_{k_1}}(t_{m_1}), G_{\rho_{k_2}, \gamma_{k_2}}(t_{m_1}))Cor(G_{\rho_{k_2}, \gamma_{k_2}}(t_{m_1}), G_{\rho_{k_2}, \gamma_{k_2}}(t_{m_2})). \end{aligned} \quad (16)$$

With all the 3 different types of correlations calculated using either distribution-based prediction or data-driven estimation, the two sets of correlation matrices are obtained under H_0 and H_1 .

3.2 | Type I error: boundaries

We introduce boundary vector $\mathbf{g} = [g(t_1), \dots, g(t_M)]'$ for M stages including a final stage and $M - 1$ interim stages. To control type I errors at all stages, we utilize a monotone increasing error spending function $\alpha(v)$ with $v \in [0, 1]$, $\alpha(0) = 0$ and $\alpha(1) = \alpha^{17}$. Suppose that we monitor the information fractions at $0 = t_0 < t_1 < \dots < t_M = \tau$ satisfying $IF_{\rho_k, \gamma_k}(t_m, \tau) = v_m$, where $0 = v_0 < v_1 < \dots < v_M = 1$ are pre-defined and w_{ρ_k, γ_k} is one of the WLRTs in the combo. $\alpha(v)$ controls type I error spent at each stage via step-wise equations for stage $m = 1, \dots, M$,

$$P(G_{max}(t_j) \leq g(t_j), j = 1, \dots, m-1, G_{max}(t_m) > g(t_m) | H_0) = \alpha(v_m) - \alpha(v_{m-1}). \quad (17)$$

The boundary values \mathbf{g} can be obtained through solving the multivariate normal distribution with mean 0, and variance matrix Σ_0 with all the diagonal entries to be 1, and off-diagonal correlation entries computed following Subsection 3.1.

3.3 | Power: sample size

The sample size calculation is based on the asymptotic distribution of the multivariate normal distribution under H_1 . With all the boundaries decided in Subsection 3.2, we control the power so that

$$P(G_{max}(t_j) \leq g(t_j), j = 1, \dots, M | H_1) = \beta. \quad (18)$$

For group sequential test, sample size calculation precedes the trial. we will obtain the sample size according to predicted mean $[\tilde{\mu}(t_1)', \dots, \tilde{\mu}(t_M)']'$ and variance matrix $\tilde{\Sigma}_1$.

3.4 | A complete design

The complete design includes 3 steps as depicted in Figure 1. First, one will need to plan the test by defining the hypotheses H_0 and H_1 or their survival curves, K WLRTs within the combo, $M - 1$ interim stages and the stopping rule. The stopping rule is usually dependent on the information fraction of one of the WLRTs in the combo, i.e., stopping at $IF_{\gamma_k, \rho_k}(t_m) = v_m$ for m^{th} test if in the previous $m - 1$ stages we fail to reject H_0 . The correlation matrices can be approximated using either prediction or estimation approaches.

Prediction includes stochastic method and exact method, whereby the former would apply to all kinds of survival functions and also consider the changing at-risk proportion of treatment group, while the latter treats this proportion a constant value (denoted to be p) for formulas in Appendix 2. The estimation approach is entirely data-driven, following (3) and (13).

The stopping times can be predicted according to the predicted information fractions at each time point, and thus obtaining the distributions of the multivariate test statistics under both hypotheses. As follows, the boundaries at each stage and sample size can be predicted as well. Moreover, once we start the trial, data are collected, and the correlation matrix can be estimated accordingly using (3). Therefore, instead of using the predicted correlations, one can also estimate the correlation matrices for boundary and sample size calculation, in order to ensure that the type I errors can still be controlled when the assumed survival distributions, censoring process, or accrual procedure are violated in practice.

4 | SIMULATION STUDIES

We used the two-piece exponential provided in Appendix 2 as an example to demonstrate the performance of our proposed approach. The event times from the control arm is following an exponential distribution with rate $\lambda = \log(2)/6$ (median survival: 6 months), while the event times from the treatment arm were generated following a two-piece exponential with its hazard changing from λ to $\theta\lambda$ at after $\epsilon = 2$ months of follow-up. When $\theta = 1$, the two-piece exponential is reduced to a constant exponential as the control group. To strictly follow the distribution suggested in (1) with $Q = 2$, we have $\Theta_0 = \{1, 1\}$ for H_0 and $\Theta_1 = \{1, \theta\}$ for H_1 , where $\theta \in (0, 1)$ and $\epsilon_1 = \epsilon$, which is equivalent to (B4). Simulations under different scenarios were carried out to evaluate the proposed method using either the prediction or estimation methods under a reasonable range of effective post-delay treatment effects ($\theta \in [0.5, 0.7]$) under H_1 . To begin, we generated data following uniform accrual within time interval $[0, R]$, where $R = 14$; and with a probability $p = 0.5$ the subjects were randomly assigned to the treatment arm. All the studies were expected to end at time $\tau = 10$. We included two Fleming-Harrington weights for a maxcombo test $G_{max}(t) = \max(G_{0,0}(t), G_{0,1}(t))$ with two stopping stages: the interim and the final. Note that $G_{0,1}(t)$ should be more powerful than $G_{0,0}(t)$ in presence of a delayed treatment effect. In practice, however, the existence of such delayed effect is generally unknown. Moreover, its severity is hard to predict, thus incorporating more WLRTs can potentially provide better robustness. In the following simulations, we only focus on one-sided tests, with their type I error controlled at level $\alpha = 0.25$ and sample size targeting power $1 - \beta = 0.9$ respectively. All the simulations have been repeated 200,000 times for type I error evaluation, and 50,000 times for power evaluation.

The stopping times were decided according to the information fraction of the SLRT or $G_{0,0}$, namely the surrogate information fraction in Hasegawa¹⁴. We stop for an interim analysis at t_{int} when $0.6d$ events were observed, and terminate the study for a final analysis at t_{fin} when d events were observed, where d is the total number of events we need. In particular, the stopping

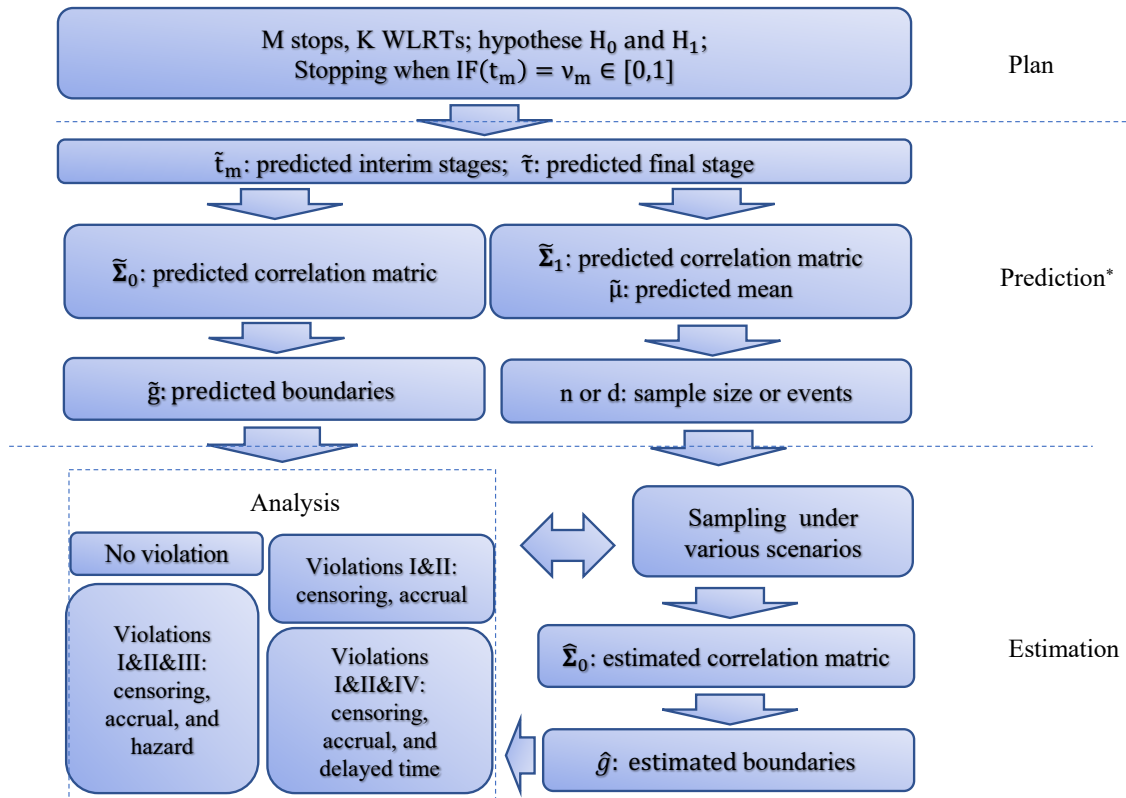


FIGURE 1 A flow-chart to describe the procedure of the proposed simulation-free GS-MC design. The superscript “*” indicates that the correlation matrices can be predicted using both the stochastic and exact approaches, while the mean ($\tilde{\mu}$) is predicted using stochastic approach to enjoy a more precise approximation. The “analysis” stage is when we conducted the maxcombo tests under various scenarios with or without assumption violations, and the output of this step is the decision to either reject or accept H_0 , which can be summarized as type I error and power in simulations. The arrows between the blocks indicate directions of the information flow.

times (t_{int} and t_{fin}) can be predicted by solving $D_{\Theta}^*(t_{int}) = 0.6D_{\Theta}^*(\tau)$ and $D_{\Theta}^*(t_{fin}) = D_{\Theta}^*(\tau)$, where $\Theta = \Theta_1$ under the alternative, and $\Theta = \Theta_0$ under the null. Note that the two sets of stopping times can differ under different hypotheses, and thus the predicted correlation matrices ($\tilde{\Sigma}_0$ and $\tilde{\Sigma}_1$). The mean of the test statistics under H_0 is $\mathbf{0}_4$, but is $[\tilde{\mu}(t_{int})', \tilde{\mu}(t_{fin})']'$ under H_1 . We obtained the predicted boundaries \tilde{g} and sample sizes d or n based on the predicted mean and correlation matrices. We can also predict the stopping times and subsequently the correlation matrices using the exact-prediction method given in Appendix 2. Alternatively, the boundaries $\hat{g}(t)$ can be updated according to the data by calculating the estimated correlation matrix $\hat{\Sigma}_0$ following (3) and (13). We used R package `mvtnorm`¹⁸ for the boundary calculation. Since it is seed-dependent, we each time generated 5 replicates, and keep the median of them as output value. All the prediction and estimation methods proposed in this report have been established in an R package which is currently available on Github (lilywang1988/IAfrac).

First, we tested various post-delay hazard ratios with only administrative censoring and correctly specified survival functions, in consistence with the assumptions given in Hasegawa¹⁰. All results were summarized in Table 1, where GS-WLRT denotes group sequential design with a WLRT $G_{0,1}(t)$, GS-SLRT denotes group sequential design with SLRT $G_{0,0}(t)$, and GS-MC denotes group sequential design with a maxcombo test of $G_{0,1}(t)$ and $G_{0,0}(t)$. Note that since all the tests were in group sequential

TABLE 1 The rejection probabilities under the null hypothesis denoted by H_0 (type I error) and under the alternative hypothesis H_1 (power) when censoring, accrual, and survival functions are correctly specified. Prefixed “GS” for the test names was eliminated here for simplicity.

Test	Stage	$\theta = 0.7$		$\theta = 0.6$		$\theta = 0.5$	
		H_0	H_1	H_0	H_1	H_0	H_1
WLRT	combined	0.0260	0.9143	0.0262	0.9140	0.0269	0.9137
	interim	0.0051	0.4082	0.0052	0.4039	0.0055	0.3983
SLRT	combined	0.0251	0.8272	0.0252	0.8206	0.0246	0.8103
	interim	0.0051	0.2487	0.0049	0.2355	0.0050	0.2283
MC (naive)	combined	0.0384	0.9279	0.0388	0.9273	0.0390	0.9258
	interim	0.0082	0.4346	0.0082	0.4282	0.0085	0.4213
MC (pred-sto)	combined	0.0251	0.8970	0.0253	0.8962	0.0255	0.8948
	interim	0.0050	0.3691	0.0051	0.3620	0.0054	0.3579
MC (pred-exa)	combined	0.0252	0.8972	0.0253	0.8963	0.0255	0.8950
	interim	0.0050	0.3693	0.0051	0.3621	0.0054	0.3582
MC (est)	combined	0.0252	0.8972	0.0253	0.8966	0.0255	0.8952
	interim	0.0050	0.3693	0.0051	0.3622	0.0054	0.3581

designs, we eliminated the prefix ‘GS’ in the summary tables. In GS-MC, we consider the naive method with boundaries that are identical to the other two univariate tests GS-WLRT and GS-SLRT, which are stopped according to the information fraction of SLRT (namely the surrogate information fraction in¹⁴). The boundaries for the other three GS-MC methods were computed from the prediction (stochastic or exact) and the estimation methods. As expected, in presence of a delayed treatment effect, GS-WLRT provides a better power than GS-SLRT, and their type I errors (0.0259 – 0.0268) were obviously higher than the nominal value 0.025 since the surrogate information fraction was not reflecting the true correlation between the two stopping times for WLRT, thus the boundaries for GS-SLRT were not appropriate for GS-WLRT. The naive GS-MC appeared to perform better with its power than WLRT, but its type I error (≈ 0.04) was not controlled.

There does not seem to exist obvious difference comparing the performance between the 3 proposed approaches, though the estimation approach had a slightly better power than the other two predicted methods with their type I error controlled similarly. The stochastic prediction does not limit its survival function to piece-wise exponential distributions, and is able to handle all difference kinds of survival functions. Its flexibility seems not improve its performance in comparison with the exact prediction approach, possibly because its prediction on the stopping times are not as accurate as those using exact prediction. All the three proposed approaches work much better than any of the naive methods in terms of controlling the type I error and power. By increasing the post-delay separation through θ , the type I error is increasing to be slightly higher than the nominal value 0.025, and the powers of both the interim stage and the two stages combined were decreasing. There could be mainly two explanations for this phenomenon: first, the accrual sample size is decreasing from $n = 927$ ($d = 597$) to $n = 274$ ($d = 166$) when the hazard ratio was decreasing from $\theta = 0.7$ to $\theta = 0.5$, thus the tails of the distribution for the test statistic became heavier than those from a normal distribution; second, the increasing treatment effect may cause a more serious violation of the independent increment assumption, and thus damages the approximation accuracy.

Then we tested different special cases with some of the assumptions, e.g., uniform accrual, administrative censoring, correctly specified survival hazards and delayed time, were violated. For violation I, the accrual is no longer uniform with a monthly accrual rate $n/14$ subjects, but instead is $n/70$, $2n/70$, $3n/70$, $4n/70$ for the first 4 months, and then $6n/70$ for rest 10 months. In presence of violation I, still there are n subjects enrolled, but the accrual rate is increasing for the first 4 months before being stabilized. For violation II, censoring is not limited to a shared administrative censoring, but can differ between treatment arms. In particular, we generated censoring time following exponential distributions with a yearly censoring proportion 20% for the treatment group and 10% for the control group. For violation III, the true median survival time for the control group is 12 months, other than the presumed 6 months. For violation IV, the separation occurs at 6 months after the enrollment, instead of the predefined 2 months. The results under various post-delay treatment hazard ratios under violations I and II (I&II) are summarized in Table 2, those with additional violation III (I&II&III) are in Web Table 1, and those with additional violation

IV (I&II&IV) are in Web Table 2. Their corresponding correlation matrices can be found in Web Tables 3-6, and their subset of results for $\theta = 0.6$ with or without violations I&II are in Table 3.

In Table 2, it turns out that all the three proposed approaches are quite robust to misspecifications of the accrual process and the censoring mechanism. The average stopping times (t_{int}, t_{fin}) were larger than those from Table 1, to collect enough events (information) in presence of an additional censoring mechanism. The detection power is even better than Table 1, probably because a longer awaiting before ending the study enable to collect more information about the late departures. Similar to the results without violations in Table 1, estimation approach has slightly better power than the two prediction methods, with all their type I error controlled similarly. Note that since the subjects are enrolled slower than those with uniform enrollment in Table 1 at the early stage, the power is generally smaller at the interim stage.

Other additional violations were considered in the Web Tables 1-2. If there exist an additional violation that the event hazard $\lambda = \log(2)/12$ is wrongly specified to be $\lambda = \log(2)/6$ (I&II&III), awaiting time to observe enough events according to the information fraction would be longer than those without violation III in Tables 1-2, and thus producing a higher power for delayed departures according to Web Table 5. Or when the delayed effect time $\epsilon = 6$ was misspecified to be $\epsilon = 2$ in addition to the violations in censoring and accrual (I&II&IV), the power would become much lower than the expected value according to Web Table 6, since the required sample sizes to achieve the nominal power were largely underestimated. Among all the combinations of violations we tested, it seems that the type I errors were not affected much, while the powers were affected depending on the degree of violations of the model assumptions.

To take a closer look at whether the correlation matrices were accurately approximated and how they were affected by the violations, we compared correlations computed using the prediction and estimation approaches with or without violations I&II in Table 3 of $\theta = 0.6$ and Web Tables 3-4, and treated the empirical correlations from the simulated data as gold standard. When there is no assumption violation, none of the correlations has more than 5% difference from the gold standard (Table 3 and Web Table 3). Only the predicted $\widetilde{cor}(G_{0,1}(t_{int}), G_{0,1}(t_{fin}))$ and $\widetilde{cor}(G_{0,0}(t_{int}), G_{0,1}(t_{fin}))$ were over 5% different from the gold standard correlations under H_1 (Table 3 and Web Table 4), possibly because the violations in censoring and accrual mechanism affect the prediction of the stopping times, thus the predicted correlations are not reflecting the true correlation within the two stopping times in $G_{0,1}(t)$. Note that $cor(G_{0,0}(t_{int}), G_{0,1}(t_{fin}))$ is approximated by the product of $cor(G_{0,1}(t_{int}), G_{0,1}(t_{fin}))$ and $cor(G_{0,0}(t_{int}), G_{0,1}(t_{int}))$ following (16). In presence of violations I&II&III, the predicted correlations for $cor(G_{0,1}(t_{int}), G_{0,1}(t_{fin}))$ and $cor(G_{0,0}(t_{int}), G_{0,1}(t_{fin}))$ would suffer from a severe bias with over 25% difference from the gold standard values. Misspecification of the delayed time, on the contrary, did not affect the correlation matrices much. The estimation method provides most accurate correlation approximations, and the correlations predicted via stochastic method is slightly more accurate than those via exact prediction method. The type I errors, however, seem not being affected much by the correlation matrices. We checked the boundaries predicted and estimated under different violation combinations and found that their changes were extremely small (< 0.003 in magnitudes), implying that slight bias in the two correlations related to WLRT did not impose considerable influence on the boundary calculation under H_0 . It is entirely possible that when there are more candidate tests included and more stopping stages in the GS-MC study, these violations become more .

In order to evaluate the gains of using maxcombo in group sequential designs, we computed the required samples sizes (14). The results were presented in Figure 2 in terms subject counts (n) and observed event counts (d). We consistently followed the identical setting proposed for Table 1 without any assumption violations, except that we fixed $\theta = 0.6$ and changed the delayed time ϵ spanning the time interval $[0, 5]$. In Figure 2, we plotted three curves: one for the maxcombo test of $G_{0,0}(t)$ and $G_{0,1}(t)$, and the other two for their respective univariate tests. The results demonstrate that the sample sizes needed by a maxcombo test is always slightly higher but quite close to the most powerful test in the combo (i.e. $G_{0,0}(t)$ when ϵ is small, and $G_{0,1}(t)$ when ϵ is large), which is much smaller than the other tests. Hence, employing maxcombo in practice can largely reduce the required sample size and improve the testing robustness.

5 | DISCUSSION

In this report, we proposed a general framework of group sequential design using maxcombo tests or GS-MC. The proposed design is completely simulation-free, and is able to effectively control the type I error and obtain sample size to achieve the power we need. We developed two prediction methods that are dependent on the assumed distributions under the two hypotheses H_0 and H_1 , and one estimation method which is completely data-driven. We demonstrated in our simulation studies that proposed

TABLE 2 The rejection probabilities under the null hypothesis denoted by H_0 (type I error) and under the alternative hypothesis H_1 (power) when censoring and accrual are misspecified. Prefixed “GS” for the test names was eliminated here for simplicity.

Test	Stage	$\theta = 0.7$		$\theta = 0.6$		$\theta = 0.5$	
		H_0	H_1	H_0	H_1	H_0	H_1
WLRT	combined	0.0259	0.9172	0.0261	0.9159	0.0268	0.9135
	interim	0.0052	0.3747	0.0053	0.3663	0.0052	0.3569
SLRT	combined	0.0248	0.8325	0.0248	0.8224	0.0250	0.8128
	interim	0.0053	0.2156	0.0051	0.2002	0.0051	0.1917
MC (naive)	combined	0.0379	0.9293	0.0383	0.9279	0.0391	0.9252
	interim	0.0085	0.3996	0.0084	0.3883	0.0084	0.3782
MC (pred-sto)	combined	0.0246	0.9010	0.0247	0.8976	0.0256	0.8953
	interim	0.0052	0.3339	0.0052	0.3255	0.0051	0.3145
MC (pred-exa)	combined	0.0246	0.9012	0.0248	0.8976	0.0256	0.8954
	interim	0.0053	0.3342	0.0052	0.3258	0.0051	0.3147
MC (est)	combined	0.0246	0.9012	0.0247	0.8979	0.0256	0.8956
	interim	0.0052	0.3335	0.0051	0.3252	0.0051	0.3141

TABLE 3 Comparison of the correlations computed using different methods: the correlations calculated directly from the simulated samples (\overline{cor}), the predicted values using either stochastic process (\widetilde{cor}_{sto}) or exact distribution (\widetilde{cor}_{exa}), and the data-driven estimation value \widehat{cor} . The sample correlations were treated as the gold standard for comparison of other methods. In comparison with the gold-standard mean, correlations with difference more than 5% were highlighted italic, and 10% were highlighted bold.

Correlation pair		No violation		Violations I&II	
		H_0	H_1	H_0	H_1
$G_{0,1}(t_{int})$ & $G_{0,0}(t_{int})$	\overline{cor}	0.8329	0.8348	0.8261	0.8263
	$\widetilde{cor}_{sto} - \overline{cor}$	-0.0029	-0.0038	0.0040	0.0047
	$\widetilde{cor}_{exa} - \overline{cor}$	-0.0009	-0.0015	0.0059	0.0070
	$\widehat{cor} - \overline{cor}$	-0.0017	-0.0027	-0.0007	0.0006
$G_{0,1}(t_{fin})$ & $G_{0,0}(t_{fin})$	\overline{cor}	0.8452	0.8516	0.8482	0.8529
	$\widetilde{cor}_{sto} - \overline{cor}$	0.0107	0.0145	0.0176	0.0230
	$\widetilde{cor}_{exa} - \overline{cor}$	0.0120	0.0162	0.0188	0.0247
	$\widehat{cor} - \overline{cor}$	-0.0010	-0.0018	-0.0008	-0.0014
$G_{0,0}(t_{int})$ & $G_{0,0}(t_{fin})$	\overline{cor}	0.7766	0.7791	0.7763	0.7797
	$\widetilde{cor}_{sto} - \overline{cor}$	-0.0037	-0.0033	-0.0035	-0.0039
	$\widetilde{cor}_{exa} - \overline{cor}$	-0.0046	-0.0016	-0.0043	-0.0021
	$\widehat{cor} - \overline{cor}$	-0.0020	-0.0045	-0.0017	-0.0051
$G_{0,1}(t_{int})$ & $G_{0,1}(t_{fin})$	\overline{cor}	0.6457	0.6267	0.6158	0.5884
	$\widetilde{cor}_{sto} - \overline{cor}$	-0.0068	-0.0074	0.0232	<i>0.0309</i>
	$\widetilde{cor}_{exa} - \overline{cor}$	-0.0068	-0.0052	0.0232	<i>0.0331</i>
	$\widehat{cor} - \overline{cor}$	-0.0012	-0.0077	0.0000	-0.0082
$G_{0,1}(t_{int})$ & $G_{0,0}(t_{fin})$	\overline{cor}	0.6475	0.6493	0.6414	0.6454
	$\widetilde{cor}_{sto} - \overline{cor}$	-0.0060	-0.0046	0.0002	-0.0008
	$\widetilde{cor}_{exa} - \overline{cor}$	-0.0052	-0.0014	0.0009	0.0024
	$\widehat{cor} - \overline{cor}$	-0.0037	-0.0047	-0.0020	-0.0049
$G_{0,0}(t_{int})$ & $G_{0,1}(t_{fin})$	\overline{cor}	0.5375	0.5262	0.5093	0.4887
	$\widetilde{cor}_{sto} - \overline{cor}$	-0.0071	-0.0115	0.0211	<i>0.0260</i>
	$\widetilde{cor}_{exa} - \overline{cor}$	-0.0059	-0.0083	0.0223	<i>0.0292</i>
	$\widehat{cor} - \overline{cor}$	-0.0018	-0.0111	-0.0011	-0.0089

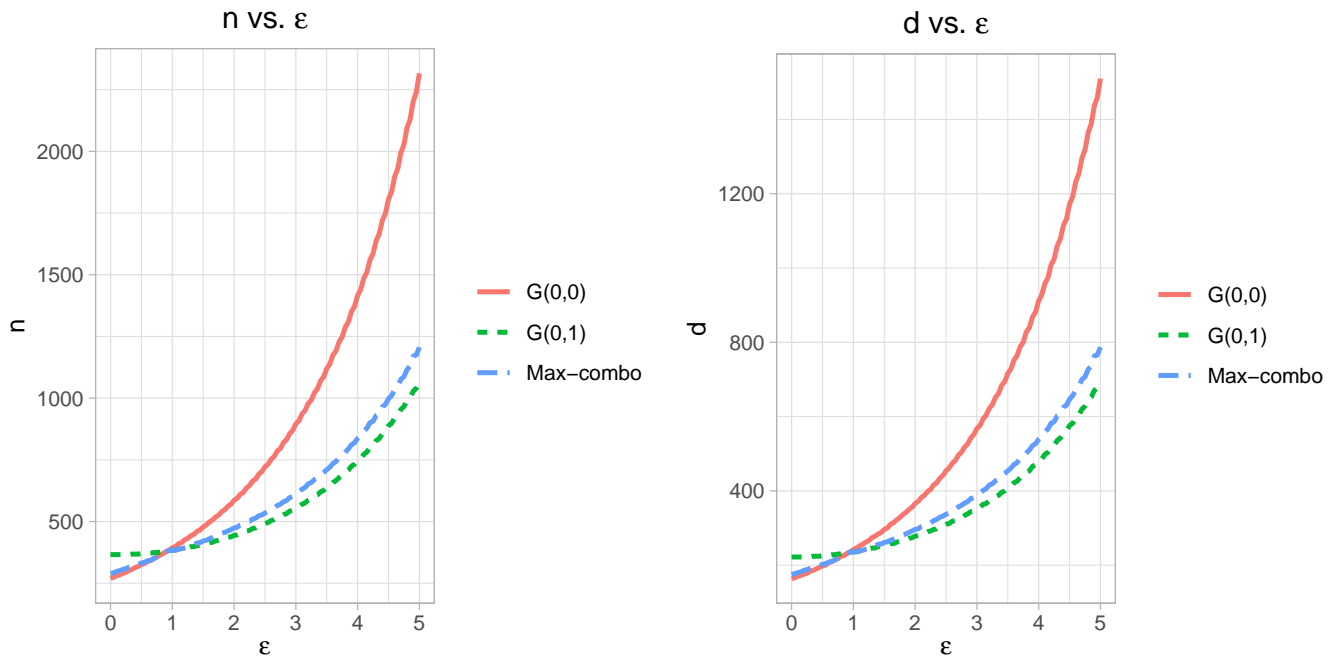


FIGURE 2 Sample sizes needed to achieve the required power $\beta = 0.9$ with different delayed effect times (ϵ) in terms of number of subjects (n) and number of events (d).

methods have strong robustness towards various violations of assumptions, including survival functions, censoring, and accrual process.

Note that among the prediction methods, the stochastic approach can fit in all kinds of survival functions while the exact approach is limited to piece-wise exponential distributions. Extensions of the exact prediction can be re-deriving the formulas in Appendix 2. In most cases, the stochastic prediction method and the exact prediction method exhibit similar performance, though the former is more flexible but also more computationally expensive than the latter.

When we were preparing the manuscript, we notice another group also developed a correlation matrix approximation method similar to ours¹⁹. They proposed to directly calculate the third type of correlations using the independent increment properties, which can be shown to be numerically identical to the ones we give in (16). The major difference between our method and their method is that their approach is not completely simulation-free, as their sample size calculation is based on simulations.

All the functions related to the proposed methods were established in an R package on GitHub (lilywang1988/IAfrac). Note that, maxcombo test without interim analysis can also be implemented by setting the number of interim stages to be 0. Though in this report we restrict our scope to the sequential design in which the sample sizes are decided before starting the trial, the proposed approach can potentially be extended to accommodate adaptive designs where the sample sizes are going to be adjusted according to observed data.

SUPPORTING INFORMATION

The following supporting information is available as part of the online article (please email lilywang@umich.edu for preprint version):

Table S1 The rejection probabilities under the null hypothesis denoted by H_0 (type I error) and under the alternative hypothesis H_1 (power) when the censoring, accrual and event hazards are misspecified. There are one interim stage and one final stage.

Table S2 The rejection probabilities under the null hypothesis denoted by H_0 (type I error) and under the alternative hypothesis H_1 (power) when the censoring, accrual and delayed time are misspecified.

Table S3 Comparison of the correlations computed using different methods without violation in accrual (I), censoring (II), survival functions (III) or delayed time (IV).

Table S4 Comparison of the correlations computed using different methods with violations I (accrual) and II (censoring).

Table S5 Comparison of the correlations computed using different methods with violations I (accrual), II (censoring), and III(event rate).

Table S6 Comparison of the correlations computed using different methods with violations I (accrual), II (censoring), and IV(delayed time).



APPENDIX

A 1: PROOF FOR THEOREM 1

Proof. This is equivalent to prove

$$E[X_1 X_2]E[X_2 X_3] = E[X_1 X_3]E[X_2^2] \quad (A1)$$

Since $X_3 = X_2 + M$ and $M \perp (X_1, X_2)$, we have the left-hand side (LHS) of (A1) to be

$$\begin{aligned} LHS &= E[X_1 X_2]E[X_2(\phi X_2 + M)] \\ &= \phi E(X_1 X_2)E(X_2^2). \end{aligned} \quad (A2)$$

The right-hand side (RHS) of (A1) is

$$\begin{aligned} RHS &= E[X_1(\phi X_2 + M)]E[X_2^2] \\ &= \phi E(X_1 X_2)E(X_2^2). \end{aligned} \quad (A3)$$

Thus the equality in (A1) holds. □

B 2: EXACT PREDICTIONS

For simplicity, we demonstrated the exact prediction for a simple case following the survival functions given in Fine²⁰ and Hasegawa¹⁰, where the control group is following an exponential distribution and the treatment group is following a two-piece exponential with delayed effect θ at ϵ :

$$S_0(s) = \exp(-\lambda s), \quad S_1(s) = \begin{cases} \exp(-\lambda s) & \text{for } s \leq \epsilon, \\ c \exp(-\theta \lambda s) & \text{for } s > \epsilon; \end{cases} \quad (B4)$$

$$f_0(s) = \lambda \exp(-\lambda s), \quad f_1(s) = \begin{cases} \lambda \exp(-\lambda s) = \lambda S_1(s) & \text{for } s \leq \epsilon, \\ \theta \lambda c \exp(-\theta \lambda s) = \theta \lambda S_1(s) & \text{for } s > \epsilon, \end{cases} \quad (B5)$$

Note that in (B4) and (B5), we have $c = \exp(-(\theta - 1)\lambda\epsilon)$ and θ as the effective post-delay hazard ratio $\theta \in (0, 1)$. If $\epsilon = 0$, (B4) and (B5) are reduced to a PH case.

According to¹⁴, the predicted variance or information is

$$\tilde{V}_{\text{exa}}(G_{\rho, \gamma}(t)) = np(1-p) \left[\int_0^t \min\left(\frac{t-s}{R}, 1\right) S(s)^{2\rho} (1-S(s))^{2\gamma} f(s) ds \right], \quad (B6)$$

Under the null hypothesis, $S(t) = S_0(t)$ and $f(t) = f_0(t)$, but under the alternative hypothesis, $S(t) = pS_1(t) + (1-p)S_0(t)$ and $f(t) = pS_1(t) + (1-p)S_0(t)$, where p is the treatment assignment probability. The major difference between \tilde{V}_{exa} and \tilde{V}_{sto} is that the at-risk proportion for the treatment group is fixed to be p in $\tilde{V}_{\text{exa}}(G_{\rho, \gamma}(t))$.

We introduce some utility functions $uv()$, $u()$ and $v()$:

$$\begin{aligned} v(t, \epsilon, k, \lambda) &= I(\epsilon \leq t - R) \int_0^t \min\left(\frac{t-x}{R}, 1\right) \exp(-k\lambda x) \lambda I(x \leq \epsilon) dx \\ &= \frac{1}{k} \{1 - \exp(-k\lambda\epsilon)\} \end{aligned} \quad (B7)$$

$$\begin{aligned} u(t, \epsilon, k, \lambda) &= I(\epsilon > t - R) \int_0^t \min\left(\frac{t-x}{R}, 1\right) \exp(-k\lambda x) \lambda I(x \leq \epsilon) dx \\ &= \frac{1}{k} \left[1 - \exp(-k\lambda(t-R)^+) \right] + \frac{R\lambda}{kR} \exp(-k\lambda(t-R)^+) \\ &\quad - \frac{(t-\epsilon)^+}{kR} \exp(-k\lambda\epsilon \wedge t) + \frac{1}{k^2 R \lambda} \left[\exp(-k\lambda\epsilon \wedge t) - \exp(-k\lambda(t-R)^+) \right], \end{aligned} \quad (B8)$$

where $(a)^+ = \max(a, 0)$ and $a \wedge b = \min(a, b)$.

$$uv(t, \epsilon, k, \lambda) = I(\epsilon > t - R)u(t, \epsilon, k, \lambda) + I(\epsilon \leq t - R)v(t, \epsilon, k, \lambda) \quad (\text{B9})$$

Based on the basic utility functions, there are some other advanced utility functions, $h_1()$, $h_0()$ and $\tilde{h}()$, for the variance/information prediction under the alternative hypothesis:

$$\begin{aligned} h_1(t, k_1, k_2) &= -\int_0^t \min\left(\frac{t-x}{R}, 1\right) S_1(x)^{k_1} S_0(x)^{k_2} dS_1(x) \\ &= uv(t, \epsilon, k_1 + k_2 + 1, \lambda) + \\ &\quad c^{k_1+1} \theta \{u(t, t, \theta(k_1 + 1) + k_2, \lambda) - uv(t, \epsilon, \theta(k_1 + 1) + k_2, \lambda)\} \end{aligned} \quad (\text{B10})$$

$$\begin{aligned} h_0(t, k_1, k_2) &= -\int_0^t \min\left(\frac{t-x}{R}, 1\right) S_1(x)^{k_1} S_0(x)^{k_2} dS_0(x) \\ &= uv(\tilde{t}, k_1 + k_2 + 1, \lambda) + \\ &\quad c^{k_1} \{u(t, t, \theta k_1 + k_2 + 1, \lambda) - uv(t, \epsilon, \theta k_1 + k_2 + 1, \lambda)\} \end{aligned} \quad (\text{B11})$$

$$\begin{aligned} \tilde{h}(t, k) &= -\int_0^t \min\left(\frac{t-x}{R}, 1\right) S^k(x) dS(x) \\ &= -\int_0^t \min\left(\frac{t-x}{R}, 1\right) \sum_{i=0}^k \binom{k}{i} p^i (1-p)^{k-i} S_1^i(x) S_0^{k-i}(x) d[pS_1(x) + (1-p)S_0(x)] \\ &= \sum_{i=0}^k \binom{k}{i} p^{i+1} (1-p)^{k-i} h_1(t, i, k-i) + \sum_{i=0}^k \binom{k}{i} p^i (1-p)^{k-i+1} h_0(t, i, k-i) \end{aligned} \quad (\text{B12})$$

The the predicted variance under the null hypothesis using the exact assumed distributions is

$$\tilde{V}_{\text{exa}}(G_{\rho, \gamma}(t)) = np(1-p) \times \begin{cases} u(t, t, 1, \lambda) & \text{for } \rho = 0, \gamma = 0; \\ u(t, t, 3, \lambda) & \text{for } \rho = 1, \gamma = 0; \\ u(t, t, 1, \lambda) + u(t, t, 3, \lambda) - 2u(t, t, 2, \lambda) & \text{for } \rho = 0, \gamma = 1; \\ u(t, t, 3, \lambda) + u(t, t, 5, \lambda) - 2u(t, t, 4, \lambda) & \text{for } \rho = 1, \gamma = 1. \end{cases} \quad (\text{B13})$$

The the predicted variance under the alternative hypothesis using the exact assumed distributions is

$$\tilde{V}_{\text{exa}}(G_{\rho, \gamma}(t)) = np(1-p) \times \begin{cases} \tilde{h}(t, 0) & \text{for } \rho = 0, \gamma = 0; \\ \tilde{h}(t, 2) & \text{for } \rho = 1, \gamma = 0; \\ \tilde{h}(t, 0) + \tilde{h}(t, 2) - 2\tilde{h}(t, 1) & \text{for } \rho = 0, \gamma = 1; \\ \tilde{h}(t, 2) + \tilde{h}(t, 4) - 2\tilde{h}(t, 3) & \text{for } \rho = 1, \gamma = 1. \end{cases} \quad (\text{B14})$$

The predicted covariance values $\widetilde{Cov}_{\text{exa}}(G_{\rho_1, \gamma_1}(t), G_{\rho_2, \gamma_2}(t))$ can be obtained following the similar strategy using $u()$ and $\tilde{h}()$ functions, by changing the squared weight of B6 to $S(t)^{\rho_1 + \rho_2} (1 - S(t))^{\gamma_1 + \gamma_2}$.

The formulas above can be easily extended to accommodate survival functions with multiple exponential pieces.

References

1. Reck M, Rodríguez-Abreu D, Robinson AG, et al. Pembrolizumab versus chemotherapy for PD-L1–positive non–small-cell lung cancer. *New England Journal of Medicine* 2016; 375(19): 1823–1833.
2. Mok TS, Wu YL, Kudaba I, et al. Pembrolizumab versus chemotherapy for previously untreated, PD-L1-expressing, locally advanced or metastatic non-small-cell lung cancer (KEYNOTE-042): a randomised, open-label, controlled, phase 3 trial. *The Lancet* 2019; 393(10183): 1819–1830.
3. Mick R, Chen TT. Statistical challenges in the design of late-stage cancer immunotherapy studies. *Cancer immunology research* 2015; 3(12): 1292–1298.
4. Harrington DP, Fleming TR. A class of rank test procedures for censored survival data. *Biometrika* 1982; 69(3): 553–566.
5. Gehan EA. A generalized Wilcoxon test for comparing arbitrarily singly-censored samples. *Biometrika* 1965; 52(1-2): 203–224.
6. Tarone RE, Ware J. On distribution-free tests for equality of survival distributions. *Biometrika* 1977; 64(1): 156–160.
7. Schoenfeld D. Sample-size formula for the proportional-hazards regression model. *Biometrics* 1983; 39(2): 499–503.

8. Schoenfeld D. The asymptotic properties of nonparametric tests for comparing survival distributions. *Biometrika* 1981; 68(1): 316–319.
9. Lee JW. Some versatile tests based on the simultaneous use of weighted log-rank statistics. *Biometrics* 1996: 721–725.
10. Hasegawa T. Sample size determination for the weighted log-rank test with the Fleming–Harrington class of weights in cancer vaccine studies. *Pharmaceutical statistics* 2014; 13(2): 128–135.
11. Lakatos E. Sample sizes based on the log-rank statistic in complex clinical trials. *Biometrics* 1988: 229–241.
12. Lee SH. On the versatility of the combination of the weighted log-rank statistics. *Computational Statistics & Data Analysis* 2007; 51(12): 6557–6564.
13. Duke-Margolis Health Policy Center . Public Workshop “Oncology Clinical Trials in the Presence of Non-Proportional Hazards”: [https : //youtu.be/npufYAHeoxk](https://youtu.be/npufYAHeoxk). 2018.
14. Hasegawa T. Group sequential monitoring based on the weighted log-rank test statistic with the Fleming–Harrington class of weights in cancer vaccine studies. *Pharmaceutical statistics* 2016; 15(5): 412–419.
15. Tsiatis AA. The asymptotic joint distribution of the efficient scores test for the proportional hazards model calculated over time. *Biometrika* 1981; 68(1): 311–315.
16. Luo X, Mao X, Chen X, Qiu J, Bai S, Quan H. Design and monitoring of survival trials in complex scenarios. *Statistics in medicine* 2019; 38(2): 192–209.
17. Gordon Lan K, DeMets DL. Discrete sequential boundaries for clinical trials. *Biometrika* 1983; 70(3): 659–663.
18. mvtnorm pR. <https://cran.r-project.org/web/packages/mvtnorm/index.html> (Last accessed Sept 20, 2019; version: 1.0.11). 2019.
19. Roychoudhury S, Anderson KM, Ye J, Mukhopadhyay P. Robust Design and Analysis of Clinical Trials With Non-proportional Hazards: A Straw Man Guidance from a Cross-pharma Working Group. *arXiv preprint arXiv:1908.07112* 2019.
20. Fine GD. Consequences of delayed treatment effects on analysis of time-to-event endpoints. *Drug information journal* 2007; 41(4): 535–539.